Methods in Ecology and Evolution

BRITISH ECOLOGICAL SOCIETY

Methods in Ecology and Evolution 2016 doi: 10.1111/2041-210X.12670

Terrestrial photogrammetry: a non-destructive method for modelling irregularly shaped tropical tree trunks

Sébastien Bauwens[1]*, Adeline Fayolle[1], Sylvie Gourlet-Fleury[2], Leopold Mianda Ndjele[3], Coralie Mengal[4] and Philippe Lejeune[4]

[1]*TERRA Research Centre, Central African Forests, Gembloux Ago-Bio Tech Université de Liège, Passage des déportés 2, 5030 Gembloux, Belgium;* [2]*UPR Bsef, CIRAD, F-34398 Montpellier, France;* [3]*Département d'Ecologie et de Gestion des ressources végétales, University of Kisangani, BP2012 Kisangani, Democratic Republic of Congo; and* [4]*BIOSE Research Unit, Gembloux Agro-Bio Tech, University of Liège, Passage des Déportés 2, 5030 Gembloux, Belgium*

Summary

1. Irregularly shaped trees including trees with buttresses, flutes or stilt roots are frequent in tropical forests. The lack of an international standard to measure the diameter of such trees leads to high uncertainties in biomass estimation, tree growth and carbon budget monitoring.

2. In this study, we developed a new method based on terrestrial close-range photogrammetry for measuring and modelling irregular stems. This approach is cheap and easy to implement in the field as it only requires a camera and a graduated rod. We validated the approach with destructive cross-section measurements along the stem of three buttressed trees. To demonstrate the broader utility of this method, we extended the validated approach to 43 additional trees belonging to two species: *Celtis mildbraedii* (Ulmaceae) and *Entandophragma cylindricum* (Meliaceae). Based on the three dimensional models, we computed shape indices for each tree, and we analysed the stem morphology of the two species. Finally, we analysed some standardized predictors for the estimation of above-ground biomass.

3. We found a high concordance between diameters derived from the photogrammetric process and destructive diameter measurements along the stem for the three calibration trees. We found that *C. mildbraedii* develop much stronger irregularities than *E. cylindricum*. We also identified a large intraspecific variation in trunk morphology for *E. cylindricum*. The basal area at 1·3 m height ($D_{area130}$) seems to be a more robust predictor for biomass estimates (lowest Akaike information criterion and relative squared error) than diameter measured above buttresses (DAB) or diameter at breast height estimated from available taper model. Finally, $D_{area130}$ might be estimated with a good precision [root mean square error (RMSE) $<$ 5%] with linear model based on the field measurements DAB and the perimeter of the convex hull of the buttresses at 1·3 m height ($D_{convhull130}$).

4. In this study, we showed the high potential of the photogrammetry for measuring and modelling irregular stems. Photogrammetry could then be used as a non-destructive measurement tool to produce correction factors for standardizing the diameter of irregular stems at a reference height which is a key issue in tree growth monitoring and biomass change estimation.

Key-words: above-ground biomass, buttress, diameter above the buttresses, permanent sample plot, point of measurement, shape index, structure from motion, taper model, three dimensional modelling, tropical forest

Introduction

Tropical forests are species-rich and structurally complex ecosystems. Understanding the functioning of these ecosystems and their role in the global carbon cycle requires detailed and repeated tree measurements (Pan *et al.* 2011; Banin *et al.* 2014; Coomes, Burslem & Simonson 2014).

The most important and easiest variable to measure in the field is trunk diameter at the base of the tree. At the tree level, diameter is strongly related to the other descriptors of tree size such as total height (Feldpausch *et al.* 2011; Banin *et al.* 2012) and crown dimensions (Antin *et al.* 2013). Diameter is thus a key predictor to estimate stem and tree volume (Belyea 1931; Nogueira, Nelson & Fearnside 2006; Fayolle *et al.* 2013b) and biomass (Chave *et al.* 2005, 2014). At the tree level, diameter is a proxy of tree size, which is an important life-history trait that determines the probability of regular fruiting (Plumptre 1995). At the stand level, the distribution of diameters is used to describe stand structure (Rondeux 1993) and recovery after disturbance. Successive diameter measurements of trees in permanent sample plots enable the quantification of tree growth (Swaine, Lieberman & Putz 1987; Clark & Clark 1999), wood production (Banin et al. 2014) and forest-level carbon budgets

*Correspondence author. E-mail: bauwens.sebastien@gmail.com

(Clark 2002; Pan et al. 2011; Coomes, Burslem & Simonson 2014).

MEASURING TREE DIAMETER

In permanent forest plots, tree diameter is repeatedly measured at the same reference height (defining the 'point of measurement', POM). The international standard for POM is 'at breast height', and the corresponding diameter is called the diameter at breast height (DBH, Belyea 1931). This breast height is generally defined as 1·3 m above ground level (Bruce & Schumacher 1950; Alder & Synnott 1992), but there are still local variations (e.g. 4·5 ft in the USA and 1·5 m in Belgium). In forest inventories, special recommendations have been made for trees on slopes, leaning trees, forked trees and trees with local deformation at breast height (Forbes & Meyer 1955; Cailliez 1980; Alder & Synnott 1992; Rondeux 1993; Condit 1998; Picard & Gourlet-Fleury 2008). However, there is no standardized protocol for irregularly shaped stems such as fluted or buttressed trees and trees with stilt roots, even though they are abundant in tropical forests.

DEALING WITH TREE IRREGULARITIES

Handbooks and technical papers recommend moving the POM above the buttresses or the stilts to reach a regular part of the stem. In the case of buttressed trees, Alder & Synnott (1992) recommended using a height of at least 1 m above buttresses so that the POM can remain the same for a decade or more and does not require continual upward adjustment. In some permanent sample plots, diameter measurements have been moved up 30 cm above the buttresses (Cailliez 1980), as in Marcá Island, Brazil (Thompson *et al.* 1992), or 50 cm above the buttresses, as in Barro Colorado Island, Panama (Condit 1998), and in the Amazonian plots of the RAINFOR network (Phillips *et al.* 2015). Alternatively, focusing on tropical African forests where trees are known to achieve larger diameters (Slik *et al.* 2013) and show huge deformations at breast height (Letouzey 1982; Chapman, Kaufman & Chapman 1998), Picard & Gourlet-Fleury (2008) recommended fixing the POM at a standardized height of 4·5 m for all trees belonging to species that develop buttresses. This recommendation was adopted in Mbaïki, Central African Republic (Gourlet-Fleury *et al.* 2013), and in the Central African plots of the DynAfFor network (www.dynaffor.org). In the case of fluted trees, two contrasting options have been recommended: either selection of the POM arbitrarily above the deformation (Alder & Synnott 1992; Condit 1998) or measuring the perimeter of the convex hull of the stem at the standard 1·3 m height (Phillips *et al.* 2015).

THE NEED FOR A STANDARDIZED METHOD

The lack of a worldwide standard for measuring the reference diameter for all morphological stem types may lead to substantial misinterpretations, errors, and biases when estimating the basal area (Clark 2002), above-ground biomass (Dean, Roxburgh & Mackey 2003; Muller-Landau *et al.* 2014), tree growth (Metcalf, Clark & Clark 2009) and the carbon budget of tropical forests (Clark 2002; Cushman *et al.* 2014; Muller-Landau *et al.* 2014). Buttressed stems represent up to 80% of trees with a diameter of at least 100 cm in 20 ha in the southwest of China (He *et al.* 2012) and more than 70% of the emergent trees studied in Bangladesh (Mehedi, Kundu & Chowdhury 2012). Irregularly shaped trees account for a large proportion of uncertainty in the carbon budget of tropical forests mainly because large trees contribute significantly to carbon stock (Slik *et al.* 2013; Bastin *et al.* 2015).

MEASURING THE IRREGULAR PART OF THE TREE

To accurately measure the basal area and the volume of irregular stems, a variety of methods, including destructive and non-destructive approaches, have been proposed. Destructive methods have been used to develop allometric equations. The irregular parts of stems are logged, and the cross-sections are measured based on georeferenced photographs and digitalization of the outline of the sections (Dean & Roxburgh 2006; Fayolle *et al.* 2013a) or drawings on large sheets of paper (Nogueira, Nelson & Fearnside 2006).

Non-destructive approaches include the wire method, the convex–concave method and the terrestrial laser scanning (TLS) method. The wire method uses two wires pressed against the irregular stem to shape the cross-section. The shaped wires are then put on a wooden board with a grid, and the area of the cross-section is estimated by counting the squares enclosed within the wire (Ngomanda *et al.* 2012). Nevertheless, the flexibility of the wire and the square counting may lead to measurement errors. The convex–concave method requires various measurements of all convex (spurs) and concave parts (flutes) of the stem to finally model the trunk as an arrangement of a cylindrical element and buttress elements (Dean & Roxburgh 2006; Henry *et al.* 2010). The simplification of the stem morphology may not always be in accordance with the real volume of this irregular part (Nölke *et al.* 2015). The TLS method requires scanning of the tree from different points of view. The resulting three dimensional point cloud is then processed to extract cross-sectional areas (Nölke *et al.* 2015). The TLS method is promising but expensive, and occlusion may hide some parts of the irregularities. Instead of measuring the basal area at 1·3 m height for the irregular trunks, Cushman *et al.* (2014) proposed an alternative method based on the taper of the trees. This taper curve method requires diameter measurements of the regular part of the stem (i.e. above the buttresses) to calibrate a taper model and project that taper downward up to 1·3 m height (Cushman *et al.* 2014). This last method assumes that the equivalent regular diameter at 1·3 m height is highly related to above-ground biomass but this hypothesis has not been validated.

AIMS AND QUESTIONS

In this study, our main objective was to develop a non-destructive method for the three dimensional modelling of tree trunks

suitable for large and irregularly shaped tropical tree trunks. The approach is based on an automated close-range photogrammetric process and was validated on three destructively sampled trees. To demonstrate the broader utility of this method, we extended the validated photogrammetric workflow to 43 additional trees belonging to two species. Thanks to this approach, we achieved three specific objectives which are: (i) to identify the stem morphology variation within a species; (ii) to analyse the ontogenetic variation in stem morphology for the two species; and finally (iii) to identify suitable standardized predictor for biomass estimates of buttressed trees. To reach the last objective, we used biomass data from Fayolle *et al*. (2013a, b). Based on the promising results of the photogrammetric method, we developed practical recommendations at the end of the manuscript.

Materials and methods

THE CLOSE-RANGE PHOTOGRAMMETRIC APPROACH

Field measurements

The photogrammetric process was developed on three buttressed trees: one *Cynometra hankei* (Fabaceae, Nganga) and two *Celtis mildbraedii* (Ulmaceae, Ohia) located at the edge of the Yangambi Reserve, in northern Democratic Republic of Congo (see Kearsley *et al*. 2013 for site description). The approach was then extended to 43 additional trees over a large diameter range to demonstrate the broader utility of this method for tree and forest monitoring. The 43 additional trees include 19 *C. mildbraedii* (Ulmaceae, Ohia) with a diameter between 42 and 98 cm, and 24 *Entandophragma cylindricum* (Meliaceae, Sapelli) with a diameter between 73 and 251 cm (Table 1). All the trees were sampled in the Loundoungou permanent sample plot situated in northern Republic of Congo and part of the DynAfFor network (see Appendix S1, Supporting Information, for the site description). These two species are both common in moist Central African forests (Fayolle *et al*. 2014). The only criterion used for the selection of the trees was the DBH class, such that trees with lianas were also retained (Fig. S 2.1).

Before photographing the trees, we cleared small vegetation (stem with DBH < 3 cm and leaves) and small lianas up to 2 m high in a radius <2·5 m around the focal trees (Fig. S 2.2). For the three calibration trees, we used a digital SLR camera Nikon D90 with an 18- to 105-mm lens. We successively fixed the zoom lens with a tape at three different focal lengths (25 mm, 35 mm and 50 mm). We manually adjusted the aperture at $F = 4{\cdot}5$–9, depending on the focal length, while the other camera settings were kept automatic (focus, ISO and shutter speed). At each focal length, we took a set of photographs all around the tree following a similar image acquisition method as the 'one panorama each step' approach of Wenzel *et al*. (2013). At each footstep around the tree, we took a set of photographs with high overlap (vertical panorama) and cross-convergent images (Fig. SI2.3). The distance from the tree varied between 1 and 3 m. We used two different viewing heights for image acquisition: the head height (1·7 m) and 4 m using a stick. Before taking the photographs, we placed a vertical graduated rod beside the tree to later scale the three dimensional point cloud produced by the photogrammetric process. The same protocol was applied in the field for the 43 additional trees, but a prime lens of 16 mm was used instead of the 18- to 105-mm zoom lens, and panels of coded targets were used instead of the graduated rod (Fig. S 2.2). The coded targets were used to automate the whole photogrammetric process (more information below).

Motion stereo process

We used the motion stereo process to build the three dimensional structure of the stem. This phase encompasses three steps: the structure-from-motion (SfM) reconstruction process (step 2, Fig. 1), the scaling step (step 3, Fig. 1) and the dense multiview stereo (MVS) matching (step 4, Fig. 1).

In SfM reconstruction, interior (internal geometry of the camera such as the lens distortion model) and exterior (spatial location and direction of images) orientation parameters were computed using a feature-detection-and-description algorithm and Bundle Block Adjustment procedure (Barazzetti, Scaioni & Remondino 2010; Szeliski 2010). The end product is a sparse point cloud of the stem with the location of the cameras (Fig. 1, step 2). The sparse point cloud was then scaled using control points, which were manually placed on the graduated rod in all the images where the rod was visible. For the 43 additional trees, the scaling is based on the reference panel with coded targets which are automatically detected (Fig. S 2.2). Finally, dense MVS matching was performed to produce a three dimensional dense point cloud.

We used PHOTOSCAN Professional v1.0.4 (Agisoft LLC, St. Petersburg, Russia) for the photogrammetric workflow, in a computer with an Intel Core i7-3930K (6 × 2 cores @3·2 Ghz- turbo @3·8 GHz) with an AMD Radeon HD5450 graphics card and 32Go RAM (quad channels PC3-10700 @666 MHz CAS 9-9-9-24).

Post-processing of the three dimensional dense point cloud of the stem

The post-processing phase aims to compute the cross-section of the stem at various heights. Post-processing is divided into two steps: the creation of the stem skeleton (step 5, Fig. 1) and the delineation of the cross-sections (step 6, Fig. 1). The method for the post-processing phase differed between the three calibration trees and the 43 additional trees. A manual procedure was used for the calibration trees to ensure the results were independent of the post-processing procedure, whereas the dense point cloud of the 43 additional trees was post-processed with 3D RESHAPER v10.1.1 scripts. In both case, the methodological steps were the same and are presented below.

To create the stem skeleton, we first defined the stem axis by connecting the centres of 2-cm-thick slices distributed every 20 cm along the *z*-axis. The contours of the slices were manually digitized using a GIS software for the three calibration trees and automatically delineated for the 43 additional trees (intersection between horizontal planes and a mesh adjusted on the photogrammetric point cloud). The centre of each slice was computed as the farthest location from the edges within the polygon (Fig. S 2.4). This is specifically suited for irregular cross-sections in comparison with other methods (geometrical centre or barycentre) that may define a centre located outside the cross-section.

Based on the skeleton, cross-sections perpendicular to the stem axis were then delineated. For the calibration trees, we digitized another set of 2-cm-thick slices regularly distributed along the stem. For the 43 additional trees, the intersection between the mesh of the trunk and planes perpendicular to the trunk axis was calculated. Finally, we computed the area and perimeter of each cross-section, as well as the perimeter of the convex hull, mimicking tape measurements around the buttresses.

Table 1. Characteristics of the three validation trees and the 34 of the 43 additional trees

No.	Tree no.	Species	DAB (cm)	H_{DAB} (m)	Trunk height (m)	G_{130} (m^2)	$D_{area130}$ (cm)	$D_{ConvHull130}$ (cm)	De_{BA130}	De_V
	Tree C1	**OHIA**	**86**	***4·6***	***24***	**0·75**	**97·7**	**158·2**	**0·74**	**0·13**
	Tree C2	**OHIA**	**52**	***4***	***27***	**0·39**	**70·9**	**96·3**	**0·56**	**0·33**
	Tree C3	**NGANGA**	**71**	***3·4***	***17***	**0·54**	**83**	**122·1**	**0·59**	**0·19**
1	Tree 1	SAPELLI	100·9	*5*	*30*	1·09	118·0	0·95	0·17	0·20
2	Tree 2	OHIA	76·3	*5·1*	*29·2*	0·61	88·3	0·78	0·77	0·29
3	Tree 3	SAPELLI	124·1	*9·7*	*43*	2·13	164·8	1·26	0·67	/
4	Tree 4	OHIA	78·9	*5·1*	*29*	0·71	95·2	0·78	0·79	0·29
5	Tree 5	SAPELLI	136·1	*7·7*	*32*	2·20	167·3	1·36	0·62	0·25
6	Tree 6	OHIA	82·3	*5·5*	*30*	0·76	98·4	0·86	0·77	0·41
7	Tree 7	OHIA	57·1	*2·9*	*18*	0·31	62·8	0·68	0·32	0·25
8	Tree 8	SAPELLI	135·2	*6·5*	*45*	2·42	175·6	1·28	0·57	0·37
9	Tree 9	SAPELLI	174·9	*4*	*33*	3·68	216·4	1·58	0·27	0·28
10	Tree 10	SAPELLI	134·9	*4·5*	*25*	2·05	161·7	1·33	0·37	0·27
11	Tree 11	SAPELLI	68·9	*2·05*	*24·5*	0·42	73·3	0·59	0·05	0·27
12	Tree 12	SAPELLI	179·9	*4·5*	*34*	3·67	216·1	1·69	0·62	0·25
13	Tree 13	SAPELLI	/	*5·2*	*48*	2·88	191·6	1·69	0·49	/
14	Tree 14	SAPELLI	/	*7·7*	*27·4*	3·38	207·6	2·13	0·33	/
15	Tree 15	OHIA	/	*3·8*	*29·5*	0·66	91·6	0·83	0·73	/
16	Tree 16	OHIA	54·0	*1·8*	*19·9*	0·25	56·4	0·33	0·10	0·26
17	Tree 17	SAPELLI	113·6	*5·8*	*27*	1·51	138·6	1·17	0·52	0·24
18	Tree 18	SAPELLI	127·2	*4·6*	*26·4*	1·72	148·1	1·33	0·45	0·24
19	Tree 19	SAPELLI	104·3	*3·7*	*14*	1·16	121·3	1·01	0·08	0·24
20	Tree 20	SAPELLI	128·9	*4·5*	*24*	1·85	153·4	1·20	0·32	0·26
21	Tree 21	SAPELLI	122·4	*7·8*	*21*	2·15	165·6	1·23	0·72	0·31
22	Tree 22	OHIA	54·2	*3·3*	*29·6*	0·31	62·8	0·56	0·34	0·36
23	Tree 23	OHIA	39·8	*2·15*	*24*	0·14	41·8		0·14	0·18
24	Tree 24	SAPELLI	202·4	*7·7*	*34·7*	4·94	250·8	2·09	0·56	0·22
25	Tree 25	OHIA	74·1	*3·5*	*26·5*	0·54	82·7	0·62	0·73	0·34
26	Tree 26	OHIA	78·2	*4·5*	*30*	0·74	96·8	0·74	0·74	0·38
27	Tree 28	SAPELLI	126·1	*4·5*	*28·4*	1·67	145·9	1·27	0·29	0·20
28	Tree 29	SAPELLI	104·0	*1·99*	*28*	0·92	108·5	0·93	0·03	0·15
29	Tree 30	SAPELLI	133·1	*4·5*	*37*	1·93	156·9	1·30	0·23	0·28
30	Tree 31	OHIA	78·6	*3·8*	*28*	0·41	72·7	0·79	0·69	0·08
31	Tree 32	OHIA	76·2	*4·3*	*30*	0·67	92·4	0·80	0·62	0·29
32	Tree 33	OHIA	63·5	*4·6*	*21*	0·40	71·6	0·61	0·49	0·23
33	Tree 34	OHIA	43·7	*1·6*	*20*	0·15	44·3	0·40	0·05	0·15
34	Tree 35	SAPELLI	114·8	*5·8*	*31·8*	1·59	142·1	1·16	0·44	0·21

DAB, diameter above buttresses; H_{DAB}, height where the DAB was measured, that is 50 cm above buttresses; Trunk height, height of the stem up to the first branch; G_{130}, basal area at 1·3 m height; $D_{area130}$, diameter at breast height estimated as the diameter of a circular disc with the same area as G_{130}; $D_{ConvHull130}$, diameter of a circular disc with the same perimeter as the perimeter measured around buttresses; De_{BA130}, Basal Area Deficit of the cross-section at 1·3 m high; De_V, volume deficit. OHIA, *Celtis mildbraedii* (Ulmaceae); NGANGA, *Cynometra hankei* (Fabaceae); SAPELLI, *Entandophragma cylindricum* (Meliaceae).

Variables measured in the field are italicized while the other variables were computed from the photogrammetric process. Trees in bold are the trees used to validate the method (destructive measurements). The slash, "/", means "no value". The absence of value is due to the limitation of the photogrammetric method for these trees. Trees in bold are the trees used to validate the method (destructive measurements). The slash, "/", means "no value". The absence of value is due to the limitation of the photogrammetric method for these trees.

DESTRUCTIVE FIELD MEASUREMENTS

Before taking photographs on the three calibration trees, we marked the position of some of the future destructive measurements on the standing stem to further facilitate the validation. These trees were then felled, and the stems were cut into successive 2 m-long logs. The cross-section of each log, including the marked ones, was then estimated with photographs (Dean, Roxburgh & Mackey 2003; Nogueira, Nelson & Fearnside 2006; Fayolle *et al.* 2013a). To scale and rectify those photographs, a 40 cm × 40 cm Plexiglas grid with 5 cm × 5 cm graduations was placed on the cross-section and photographs taken (Fig. S2.4). The first 2 m of the stem were discarded because, for safety reasons, the buttresses were cut prior to felling. We rectified the photographs of the destructive cross-sections by applying a projective transformation using GIS software prior to manual digitization (see Appendix S2 for method description and quality assessment of this method). The destructive measurements on the marks were used for the validation of the photogrammetric process. Cross-sectional areas calculated from the three dimensional models were thus compared to destructive measurements at the exact same height.

DATA ANALYSIS

To estimate the accuracy of measurements extracted from the three dimensional models (photogrammetric measurements hereafter), the

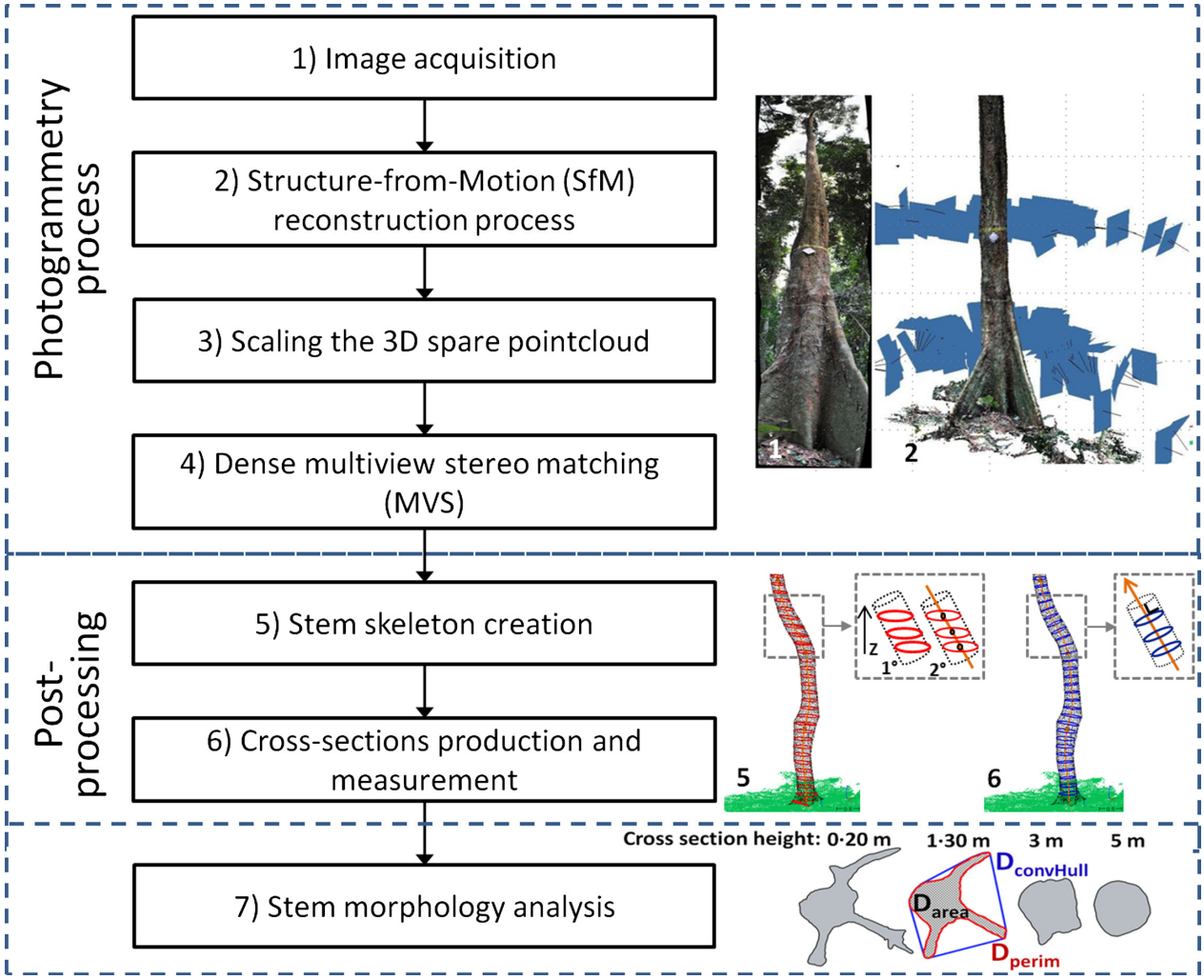

Fig. 1. Workflow of the non-destructive method for the three dimensional tree modelling suitable for large and irregularly shaped tropical trees. The main steps are (1) acquisition of photographs all around the tree, (2) location of the photographs in the three dimensional space based on the structure-from-motion process (the blue squares in sub-Figure 2 corresponds to the photographs), (3) scaling the project with reference points and (4) generating a dense three dimensional point cloud of the stem. In the post-processing phase, the tree skeleton is computed (step 5) by slicing the point cloud along the *z*-axis and estimating the centre of each cross-section. Then, measurements of cross-sections are carried out perpendicular to the skeleton (step 6). Finally, in step 7, based on the cross-sectional measurements, the stem morphology is analysed by computing shape indices and fitting taper curves. [Colour figure can be viewed at wileyonlinelibrary.com]

bias and the root means square error were first computed for the three validation trees.

Description of the stem shape

For the stem morphology analysis of the 43 additional trees, we converted our photogrammetric measurements into diameters, since diameter is more frequently used than basal area to quantify tree size in forest sciences. The area and the perimeter of the cross-sections were converted into diameter by computing the diameter of a disc with the same area (D_{area}) and the same perimeter (D_{perim}), respectively. The diameter of a disc with the same perimeter as the convex hull was also computed ($D_{ConvHull}$).

Shape indices. To better quantify the buttressed part of the 43 additional trees and to analyse ontogenetic variations, we focused on two common shape indices among the large number of indices available (Pulkkinen 2012). The Basal Area Deficit index (De_{BA}, previously used for buttressed tropical trees in Dean 2003; Ngomanda *et al.* 2012; and Nölke *et al.* 2015) is defined as one minus the ratio of the basal area of the cross-section over the area of a circular disc with the same perimeter as the cross-section (eqn 1):

$$De_{BA} = \frac{BA_{perim} - BA_{area}}{BA_{perim}} = 1 - \left(\frac{D_{area}}{D_{perim}}\right)^2, \quad \text{eqn 1}$$

with BA_{perim} the area of a disc with the same perimeter as the perimeter of the cross-section (in m²), BA_{area} the area of the cross-section (in m²), and D_{area} and D_{perim} as defined above (in cm). As a result, De_{BA} is equal to zero for a circular disc and tends to one as the cross-section becomes more irregular (Ngomanda *et al.* 2012). According to Nölke *et al.* (2015), a cross-section with a De_{BA} <0·05 can be considered circular.

The Volume Deficit (De_V) is defined as the proportion of the volume of the buttressed part of the stem that is not considered when this part

is assumed to be a cylinder with a diameter equal to the diameter above the buttresses (DAB):

$$De_V = \frac{V_b - V_{cyl}}{V_b} = 1 - \frac{(\pi/4)\,DAB^2 H_{DAB}}{V_b}, \quad \text{eqn 2}$$

with V_b, the volume of the buttressed part of the stem (in m³), V_{cyl} the volume of a cylinder with diameter equal to DAB (in m³), that is the diameter at 50 cm above the buttresses (in m), and H_{DAB} the measurement height of DAB (in m). As a result, De_V is equal to zero for a cylindrical stem and De_V tends to one as the taper of the buttressed part increases. We used the same DAB definition as Nölke *et al.* (2015) to ease comparison with their form index $f_b = V_b/V_{cyl}$.

Based on the photogrammetric data, we finally studied an objective method to determine the height of the highest buttress and the height of DAB by defining a threshold based on the difference between D_{area} and $D_{ConvHull}$.

Biomass predictors

To identify the most robust standardized predictor for biomass estimates of buttressed trees, we studied the quality of the allometric relationship between the total above-ground biomass and the following individual predictors: diameter at the standard height of 1·3 m based on the basal area measurement ($D_{area130}$) and based on the perimeter of the convex hull around the buttresses ($D_{ConvHull130}$) and the equivalent regular DBH deduced from taper model (DBH_{eq}).

We used Metcalf, Clark & Clark (2009)'s taper model to estimate the equivalent regular DBH (DBH_{eq}) as this model showed the best results compared to four other taper models on 190 buttressed stems at Barro Colorado Island, Panama (Cushman *et al.* 2014). The model is:

$$D_{i_i} = DBH_{eq} \cdot e^{-b_1(h_i - 1{\cdot}3)}, \quad \text{eqn 3}$$

with D_i the diameter (in cm) at height h_i, (in m), DBH_{eq} the equivalent regular diameter at 1·3 m (in cm), and b_1 is a parameter. We fitted the taper model with diameters measured above buttresses to deduce the DBH_{eq}. Two equivalent regular diameters at 1·3 m were deduced: DBH_{eqAll} and DBH_{eqSub}. DBH_{eqAll} is estimated by including all the diameters measured above the buttresses, whereas DBH_{eqSub} is estimated with a subset of the diameters between H_{DAB} and 10 m high as in the field protocol of Cushman *et al.* (2014).

As no destructive measurements of biomass were done in the Loundoungou permanent sample plot, the biomass data used to analyse the predictors are a subset (n = 15) of Fayolle *et al.* (2013a, b) data from south-east of Cameroon. We only selected the *E. cylindricum* trees as this is the only species for which photogrammetric data were available. We fitted the following allometric model to the biomass data:

$$Ln(AGB) = a\,Ln(D) + b\,Ln(D^2), \quad \text{eqn 4}$$

where AGB is the tree above-ground biomass (in Mg), D is one of the size predictors mentioned in the previous section (in cm), and a and b are the model parameters. In order to correct for the systematic bias induced by the log-transformation, when back-transforming the data, we applied a first-order correction factor (CF), which was calculated as follows (Baskerville 1972; Sprugel 1983).

$$CF = e^{(RSE^2/2)}. \quad \text{eqn 5}$$

Afterwards, we compared the biomass prediction of our species-specific models with the multispecies models of Fayolle *et al.* (2013a, b) and Chave et al. (2005, 2014).

Finally, we studied the relationship between $D_{area130}$ and alternative field measurements: DAB, H_{DAB} and $D_{ConvHull130}$ in order to estimate $D_{area130}$ indirectly. We fitted all possible combinations of the linear model based on these three predictors and their interactions. We also fitted power models (i.e. linear models on log-transformed data) with the most relevant combination of the predictors, but these last fits did not maintain normality in the residuals. The selection of the models was performed with the leaps routine in the R software, and the final model fitting was achieved with the package nlme. We applied a flexible weight of the variance on the models in order to avoid heteroscedasticity, and we added species effect on the residuals. The relative Root mean square error (RMSE) was computed as the RMSE divided by the mean diameter of the data set.

Results

THE PHOTOGRAMMETRIC PROCESS

We took an average of 188 photographs and spent *c.* 20 min for each calibration tree and per focal length. During the SfM step (Fig. 1, step 2), we were able to orientate and locate the photographs taken with the focal length of 25 mm, but the reconstruction process failed for the set of photographs taken with focal lengths 35 and 50 mm. The time needed for processing was around 3 h and 30 min for each tree, with 2 h spent for SfM, 20 min spent for pointing markers and other manual interventions, and 1 h spent for MVS matching. The 20 min of manual intervention was not necessary for the 43 additional trees as they were photographed with coded targets. The resulting three dimensional point cloud was composed, for each tree, of ~525 000 points at the 'medium'-quality parameter setting in the dense matching step. From the 43 trees photographed for the morphological analysis 79% were successfully oriented in the SfM step (i.e. 34 trees). The success rate might be improved by restarting the SfM process on the first poor results, but we wanted to limit manual intervention during the photogrammetric process. The main factor that could explain this first unsuccessful SfM process for some trees is the low distance between the operator and the tree during the images acquisition (distance <1·5 m to avoid clearing small to medium vegetation). The overlap between the images is then insufficient to match them.

No significant bias in diameter estimation was noticed when comparing cross-section measurements manually delineated from the three dimensional point cloud and destructive reference measurements at the exact same height (rectified photograph of the marked cross-section; bias = 0·66 cm, P = 0·073, d.f. = 6). A slight bias is noticed between measurements deduced from mesh and the destructives references (bias = 0·86 cm, P = 0·02, d.f. = 6). Nevertheless, the reference measurements based on the rectified photograph have also a limited precision and accuracy that might influence the bias reported (Appendix S2).

STEM MORPHOLOGY VARIATION

To better quantify the buttressed part of the 34 remaining trees and to analyse ontogenetic variations, we used two shape

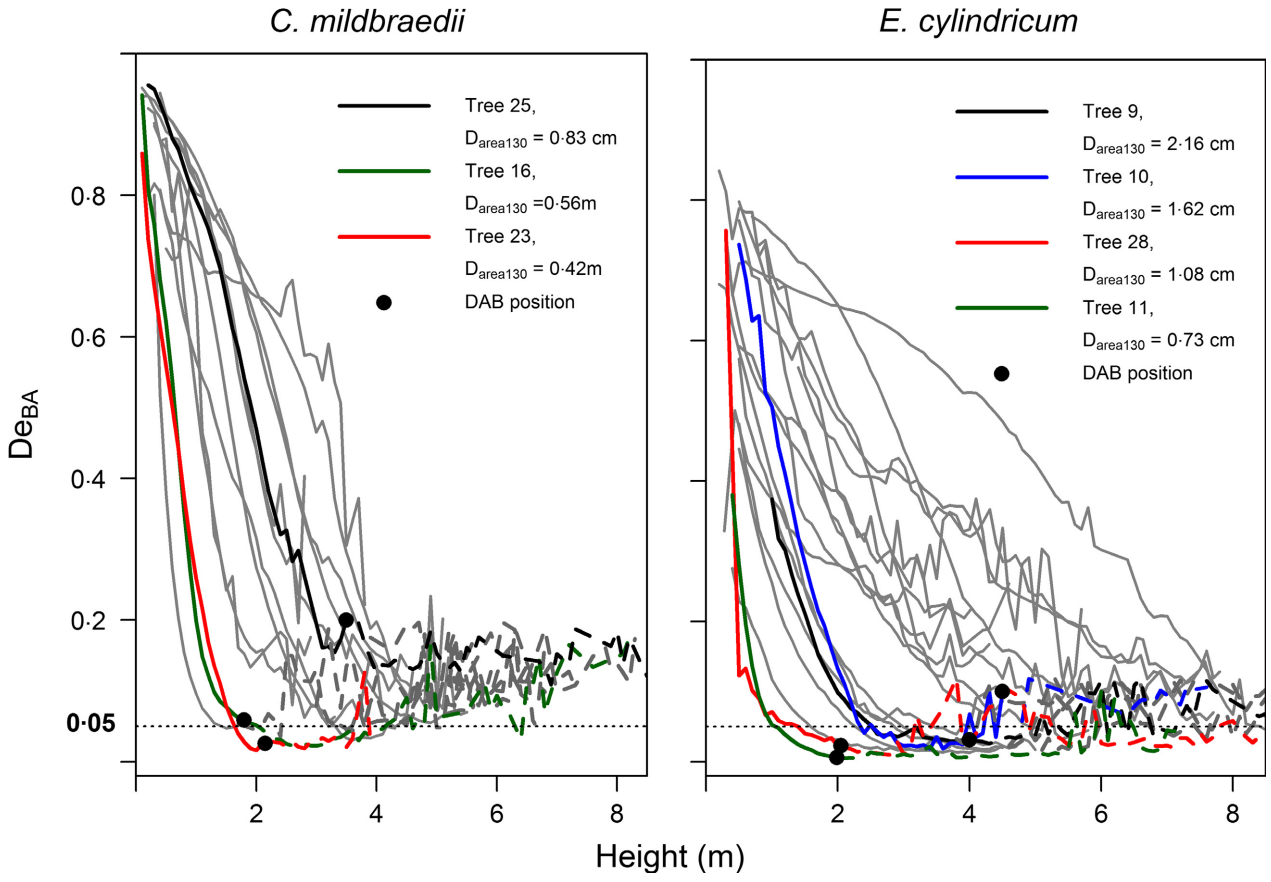

Fig. 2. Variation of the shape index DeBA (Basal Area Deficit) along the stem for 14 *C. mildbraedii*) and 20 *E. cylindricum*. The coloured lines correspond to trees with contrasted diameters, and the black dots, as well as the intersection between the solid and dashed lines, indicate the position of the diameter above buttresses (DAB). Cross-sections with a De_{BA} below the 0·05 reference value are considered circular. [Colour figure can be viewed at wileyonlinelibrary.com]

indices. The first shape index (the Basal Area Deficit: De_{BA}) strongly decreased along the stem in the first metres (i.e. the buttressed part of the stem) in both species, but tended to stabilize at 4·5 m height for *C. mildbraedii* and not before 8 m for *E. cylindricum* (Fig. 2). The trunk appeared to be much more regular above 4·5 m for most *C. mildbraedii* trees though not circular ($De_{BA} > 0{\cdot}05$, the reference value for circular cross-section).

There was extensive intraspecific variation in the development of irregularities along the stem. The intraspecific variation tended to be greater for *E. cylindricum* since some trees could be considered circular ($De_{BA} \leq 0{\cdot}05$) from 1 m height (trees 11 and 28, in red and green, respectively, in Fig. 2) while others were greatly irregular up to 8 m height. This variation was not fully attributable to tree size since the largest trees were not necessarily the most irregular ones along the stem. For instance, the large *E. cylindricum* tree 9 (in black, with a diameter of 219 cm) was circular from 2·5 m height whereas some smaller trees have strong irregularities up to 8 m.

The average De_{BA} at the DAB height is 0·08, showing that determining height of the DAB in the field is in accordance with the height where the stems turn out to be more regular. The choice of 3% threshold for the relative difference between $D_{ConvHull}$ and D_{area} seems to be a good reference value to objectively define the height of the highest buttress and increased to 5% if the tree did not reach this threshold within the 10 first metres of the stem (Table S 3.1). Finally, within the 34 trees with three dimensional data, four trees were left without information on the DAB height due to obstruction by surrounding vegetation.

When comparing tree size at 1·3 m ($D_{area130}$) to stem irregularities at 1·3 m (De_{BA130}), we found that irregularities increased with the diameter of the trees (Fig. 3). *Celtis mildbraedii* trees tended to develop much stronger irregularities than *E. cylindricum* trees for the same diameter at 1·3 m. The development rate of irregularities (slope of the relationship between De_{BA130} and $D_{area130}$) was almost six times larger for *C. mildbraedii* than for *E. cylindricum*, showing the ontogenetic difference between these two irregularly shaped tree species. The relationship between tree size and tree irregularities at 1·3 m was weaker for *E. cylindricum* ($R^2 = 0{\cdot}34$) than for *C. mildbraedii* ($R^2 = 0{\cdot}88$). This might be due to the great intraspecific variation in tree irregularities within this species as already identified along the stem (Fig. 2).

The second shape index, the Volume Deficit Index (De_V), varied between 0·08 and 0·41 among the 31 additional trees for

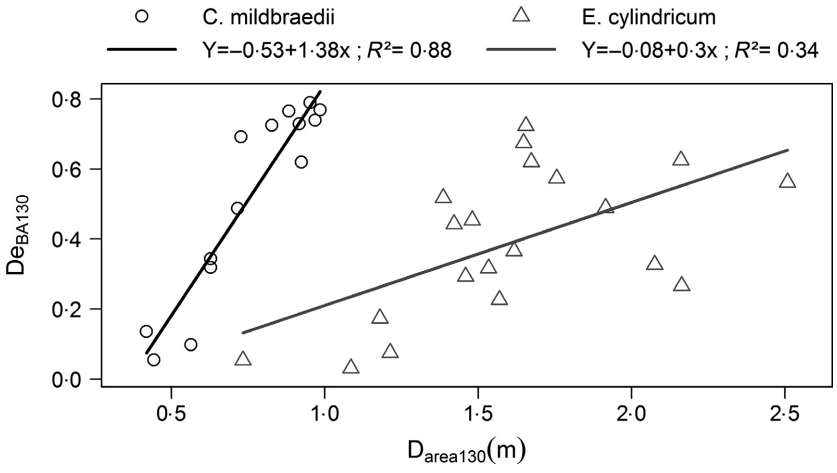

Fig. 3. Relationship between the shape index De_{BA} (Basal Area Deficit) at 1·3 m height and the diameter of a disc with the same area as the basal area at 1·3 m height ($D_{area130}$).

which the above buttress height (H_{DAB}) was attained by the three dimensional model (Table 1). We did not find any significant difference in mean De_V between the two species ($P = 0{\cdot}43$, $t = -0{\cdot}80$). The mean De_V value across all trees was 0·26 (±27%), which means that on average 26% of the volume of the buttresses is not considered when the volume is estimated as a cylinder with the diameter above buttresses (DAB). The De_V increased with DAB, indicating that the taper of the basal area of the buttressed part of the trunk increased with tree size, and this was stronger for *C. mildbraedii* than for *E. cylindricum*. The highest De_V value was observed for the largest *C. mildbraedii* (Table 1).

STANDARDIZING THE HEIGHT OF DIAMETER MEASUREMENTS

Among the biomass allometric models fitted on the 15 *E. cylindricum* from Cameroon (Fayolle *et al.* 2013a, b; Appendix S3), the model providing the best fit on biomass data was the m2 model with the predictor variable $D_{area130}$ (lowest Akaike information criterion (AIC) and relative squared error (RSE), Table 2). The m1 model based on the predictor variable DAB lost a high proportion of information compared to m2 (lowest AICw). Models using estimated DBH_{eq} from Metcalf, Clark & Clark (2009) taper model (m4 and m5) improved slightly the prediction of biomass compared to m1 as well as the model m3 which required the measurement of the perimeter around the buttresses ($D_{ConvHull130}$). These results based on a low number of samples ($n = 15$) tend to show that building biomass allometric equation with the variable $D_{area130}$ might reduce substantially the root mean square error of biomass allometric model. Moreover, using this standardized variable on existing allometric equation which were fitted with a mixed of DBH and DAB seems to reduce the important bias encountered on biomass estimates of large trees (diameter > 100 cm, Fig. 4).

The relationships between the $D_{area130}$ derived from the three dimensional models and several field measurements are shown in the Fig. 5. We found that $D_{area130}$ was best explained (lowest BIC) with the following variables: the combination of $D_{ConvHull130}$ and H_{DAB} ($D_{ConvHull130} : H_{DAB}$), the combination of DAB and H_{DAB} (DAB : H_{DAB}) and DAB (model md1 of the Table S3.3). The best model with only two variables was the model md5 with $D_{ConvHull130}$ and DAB as explanatory variables. No residual effect of species was found for these two models. The relative RMSE of the models md1 and md5 are, respectively, 4·5% (absolute RMSE of 5·8 cm) and 4·6% (absolute RMSE of 5·9 cm), and the exponents of the power model used for the residual variance are, respectively, 0·793 and 0·719.

Discussion

In this study, we found a good agreement between diameters derived from the three dimensional models and the destructive measurements along the stem for the three validation trees. Our results (RMSE <1 cm on tree diameter) were better than the ones reported in a study on small trees in boreal forests (RMSE = 2·39 cm, Liang *et al.* 2014). We therefore believe that the non-destructive approach based on close-range terrestrial photogrammetry developed in this study is an objective and accurate method that can be used to measure large and irregularly shaped tropical trees.

To illustrate the broader utility of our method, we applied the whole photogrammetric process to 43 additional trees belonging to two species. According to expectations, we found that tree irregularities decreased along the stem; and that tree irregularities at 1·3 m height increased with tree size with greater irregularities for *C. mildbraedii* than for *E. cylindricum*. The Basal Area Deficit in *E. cylindricum* trees was similar to the 0·39 mean value of 102 buttressed trees measured in Gabon (Ngomanda *et al.* 2012), while in *C. mildbraedii,* De_{BA} was far greater (0·52). We also identified a large intraspecific variation in trunk morphology for *E. cylindricum* which can, for similar diameters, be almost regular or show fully developed buttresses (Letouzey 1982; Meunier, Moumbogou & Doucet 2015).

Since the research of Chave et al. (2005, 2014) on biomass allometry, different studies aimed to improve the precision of allometric equations by adding information on crowns (e.g. mean radius of the crown or height of the crown) in their equation to reduce the high bias encountered on biomass estimates of large trees (diameter > 100 cm, Antin et al. 2013;

Table 2. Results of the regression analysis of the biomass allometric eqn (4)

Model	Predictor D	D	D^2	Intercept	AIC	AIC_w	RSE	d.f.
m1	DAB	*			−0·8	0·0008	0·202	12
m2	$D_{area130}$	***	.	*	−15·1	1·0000	0·125	12
m3	$D_{ConvHull130}$	***	**	**	−9·9	0·07	0·149	12
m4	DBH_{eqAll}	*	.	*	−3·6	0·003	0·184	12
m5	DBH_{eqSub}	***	*	**	−5·7	0·009	0·171	12

AIC, Akaike information criterion; RSE, relative squared error.
AIC_w is the relative likelihood of the models.
The asterisks refer to the significativity of the parameter: ., 0·1 < P value < 0·05; *, 0·05 < P value < 0·01; **, 0·01 < P value < 0·001; ***P value < 0·001.

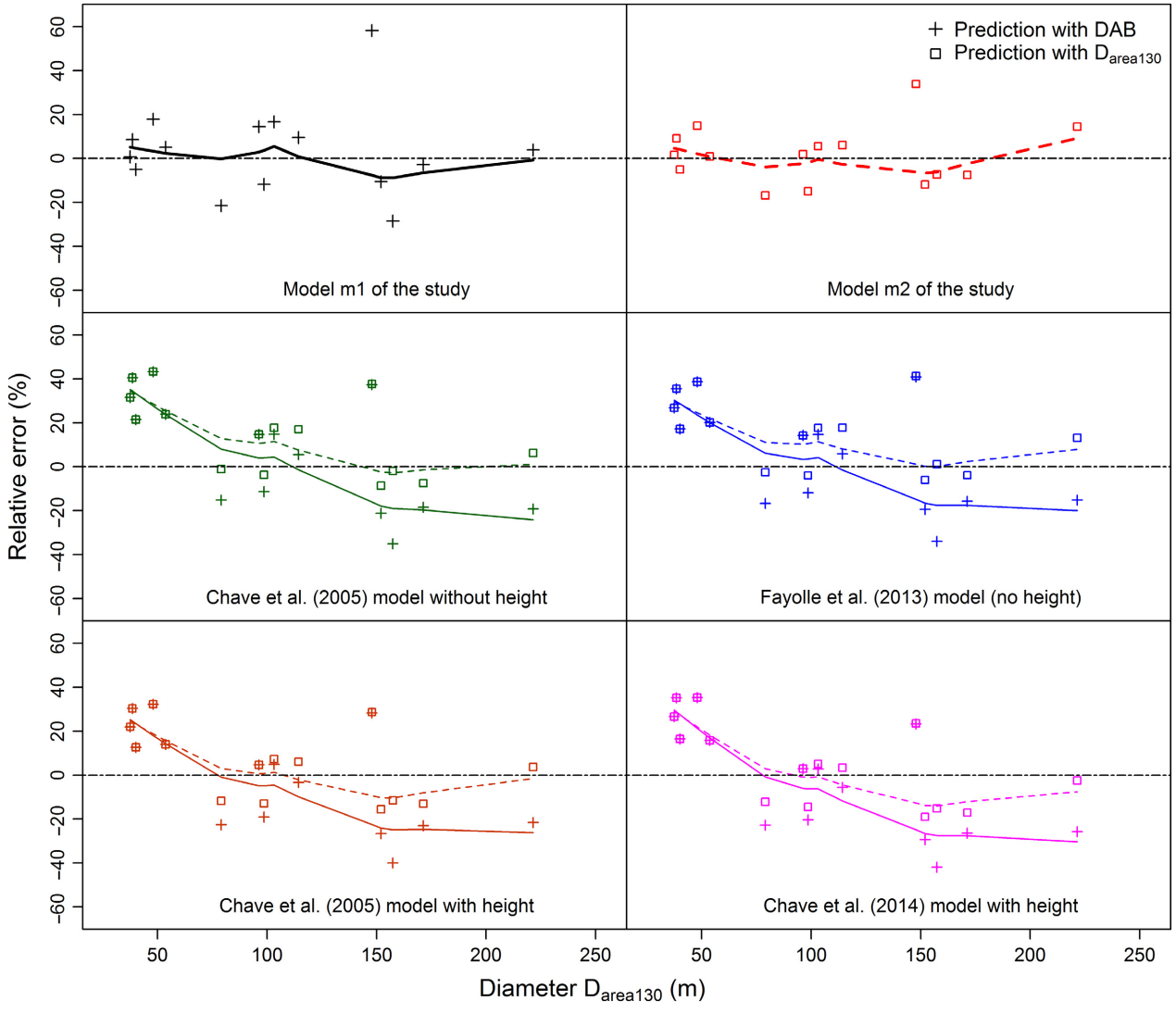

Fig. 4. Biomass error of different allometric models according to the diameter used. The model m1 is the model fitted with DAB, the model m2 is the model fitted with $D_{area130}$, the Chave et al. (2005, 2014) model without height is the model for moist forest which is fitted with a mixed of DBH and DAB data, the Fayolle *et al.* (2013a, b) model is a local multispecies model which is fitted with a mixed of DBH and DAB data, the Chave et al. (2005, 2014) model with height is the model for moist forest requiring the height in addition to diameter and basal wood density (also fitted with a mixed of DBH and DAB data) and the Chave *et al.* (2014) model with height is a model requiring the height in addition to diameter and basal wood density (also fitted with a mixed of DBH and DAB data). The solid and dashed lines are local fitted lines (loess fitting with a span of 2/3), the solid line is fitted on biomass data predicted with DAB (cross symbols) and the dashed line on biomass data predicted with $D_{area130}$ (square symbols). DAB, diameter above buttresses. [Colour figure can be viewed at wileyonlinelibrary.com]

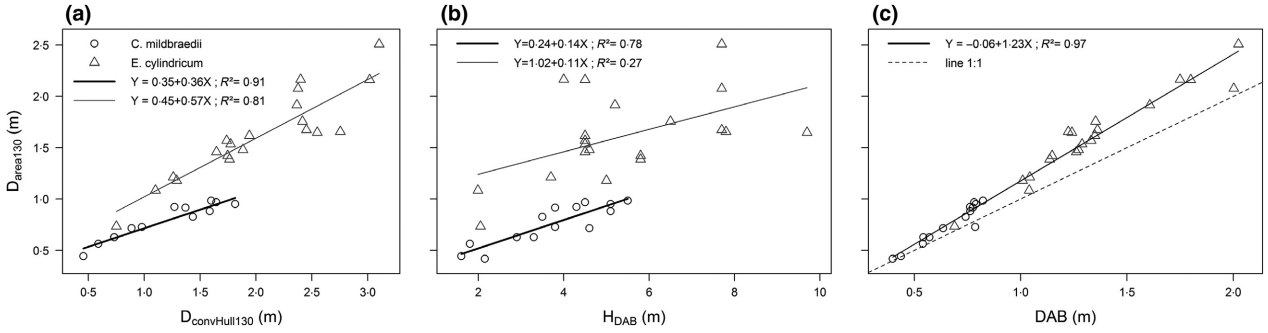

Fig. 5. Relationships between the diameter of a disc with the same area as the basal area at 1·3 m height ($D_{area130}$) and field measurements including the diameter of the convex hull measured at 1·3 m height ($D_{ConvexHull130}$) around the buttresses (a); the height of the diameter above buttresses (H_{DAB}) (b); and the diameter above buttresses (DAB) at a variable height (c).

Goodman, Phillips & Baker 2014; Ploton *et al.* 2016) . This study shows that a higher accuracy on biomass estimates might also be achieved by standardizing the diameter to $D_{area130}$ on the existing biomass allometric equations.

In addition, $D_{area130}$ standard might be predicted with a good precision (RMSE < 5%) by using statistical relationships related to easily measurable variables such as DAB and the perimeter of the convex hull of the buttresses at 1·3 m height, regardless of the species (this study, Ngomanda *et al.* 2012; Nölke *et al.* 2015). These are promising results for the standardization of diameter measurement height in permanent sample plot which is a key issue for tree growth monitoring (Metcalf, Clark & Clark 2009) and biomass estimation (Muller-Landau *et al.* 2014). The systematic use of terrestrial photogrammetry and/or terrestrial LiDAR scanning (Nölke *et al.* 2015) in tree and forest monitoring offers new opportunities to directly measure irregularly shaped trees as well as to develop correction methods to extract diameter measurements at any measurement height (e.g. taper model in Appendix S3 and models relating $D_{area130}$ with easily measurable variables). These correction methods are needed for growth comparisons between trees, within and between sites.

In comparison with terrestrial LiDAR scanning, close-range photogrammetry combines a high mobility that reduces the occlusion generated by stem irregularities and surrounding vegetation, a low cost, a high portability, and a low acquisition time, that places this approach as a new competitive tool for measuring the base of the trunks. Nevertheless, as other terrestrial remote sensing tools, low vegetation and lianas limit measurements possibilities in dense forest as in the study site. In this study, the photogrammetric process failed for 21% of the photographed trees due to non optimal acquisition, as we wanted to limit our impact on the vegetation surrounding the focal trees. Moreover, measurements up to the top of the buttresses were not possible for four of the 34 remaining trees due to the same problem. The actual technical limits of the tool are the non 100% success of the SfM process, the high computer processing time and the manual cleaning of the dense point cloud. To ensure a high rate of success of the SfM reconstruction process, some recommendations are proposed in the next section.

Recommendations

On the basis of our own experience as well as on a literature review, we make the following additional suggestions to ensure the success and quality of the photogrammetric process in tropical forests. The automatic SfM process is the most critical step in the overall photogrammetric process, and its correct achievement is not guaranteed. The success of SfM is highly related to (i) the quality of the camera gear and its lens distortion model, (ii) the image acquisition protocol (angle view and overlapping of the images), and (iii) the quality of the images acquired which should not be blurred, under/overexposed or backlighted.

CAMERA GEAR QUALITY

Low-cost uncalibrated consumer-grade digital cameras are now commonly used to build three dimensional models of well illuminated objects as buildings or statues. The most obvious examples are popular projects made and shared with the browser-based SfM software PHOTOSYNTH® (Microsoft, photosynth.net). However, it must be kept in mind that successful photogrammetric process and accurate results depend on the image quality, consistency, and uniformity. The camera should therefore have high-quality optics, a large sensor size and a high autofocus speed in low-light environment.

We succeeded in the SfM step for the three calibration trees with only the widest focal length (25 mm) because of the higher overlap between images compared to longer focal lens. In addition to a wide focal lens, a fixed lens is also recommended because of the better geometric stability than zoom lens (Shortis *et al.* 2006). We thus recommend using a prime wide angle lens (focal inferior to 35 mm). Otherwise, in compact cameras with an optical zoom, no zooming (zoom of 1×) is recommended as it is the widest angle and leads to a more stable principal distance than other zooms (Läbe & Förstner 2004).

IMAGE ACQUISITION PROTOCOL AND LENS DISTORTION MODEL

The first step of the photogrammetric process is the image acquisition. The protocol to acquire images should follow the suggestions of Wenzel *et al.* (2013) to take a panorama of the

object of interest at each step, but cross-convergent images should also be taken at each step (Fig. S2.3). Several angles of view are also recommended (e.g. one set of images taken at head height and another set taken above with a monopod for instance). Adding reference points around the tree will also increase the success of the automatic SfM process. We then suggest using a coded target around the tree which will be automatically detected and used as reference points for the SfM process (Fig. S 2.2).

As the forest is an extreme environment for the photogrammetric process (low luminosity, backlight, movement of the leaves and changing depth), any extra information that can help the SfM step are important. We observed in several photogrammetric projects that adding a precise lens distortion model as an input to the SfM step leads to successful results, though the SfM failed without lens distortion model. In order to build the lens distortion model, self-calibration of the camera is thus recommended: (i) before each image acquisition with a certain focal length, if the focal length is modified during the image acquisition campaign, or (ii) before an image acquisition campaign when using a single prime lens. The self-calibration of the camera means that we estimate intrinsic parameters of the camera based on a set of images. The estimation of these geometric characteristics, that is, the focal length (f) of the lens, the coordinates of the centre of projection of the image (xp, yp) and the radial lens distortion coefficients, is performed automatically using a photogrammetric software applications. The set of images should be capture in an illuminated scene with textured and non-flat objects (e.g. a corner of a messy desk) or on dedicated contrasted panel proposed by the photogrammetric software such as a chess board. The parameters of the camera should be the same as the parameters used in the field, more specifically the zoom and focus of the camera.

In this study, we were able to model the three dimensional structure of the stem of tropical trees up to 12 m height. The height limitation is due to the backlight of some images, and the lower resolution and higher inclination of the images of the upper part of the tree. Oblique images are not recommended in the photogrammetric process because of the shift in depth between two neighbouring pixels, which leads to a disparity gradient (Wenzel *et al*. 2013). To model the upper part of the trunk for volume or biomass estimations, the use of a large telescopic pole to raise the camera up to the top of the trunk would be needed or the use of a drone with protections around the propellers to avoid contact with the branches.

IMAGE QUALITY

In photogrammetry, a good image is an image that is not blurred, that is well exposed, and sharp. The use of automatic settings (specifically, automatic aperture, shutter speed and ISO) and automatic focus guarantees, on average, a good image quality. The various settings of each photograph are now well managed by the latest photogrammetric software.

Using autofocus during image acquisition results in a change in the optical and geometrical property of the lens between each image. According to Fraser & Al-Ajlouni (2006), changing the focus does not have a significant effect on distortion parameters. Läbe & Förstner (2004) reported a significant effect on camera calibration when changing focus in photographs closer than 0·5 m from the object. As photographs of the trunk are taken at a distance further than 0·5 m in our protocol, we would recommend focusing each picture to ensure sharpness. Finally, the diffuse light of an overcast day is recommended compared to the direct light of a sunny day.

Authors' contributions

S.B., A.D., S.G.-F. and P.L. designed the study; S.B. and C.M. conducted the fieldwork; S.B. and C.M. did most of the data analysis; S.B., A.D. and S.G.-F. wrote the manuscript and L.M.N. and P.L. supervised the research and reviewed the manuscript.

Acknowledgements

We thank the Center for International Forestry Research (CIFOR), Resources and Synergies Development (RSD) and the University of Kisangani, through the REFORCO project funded by the European Union, for their financial and logistic support. We thank also the INERA Yangambi, who hosted this study in their research area, and more specifically Henri Badjoko, for his assistance in the fieldwork. We thank the DynAfFor team for their logistic support and their assistance in the fieldwork in Congo and the CIB-Olam company, partner of the DynAfFor project, who hosts the PSP of Loundoungou. Part of S. Bauwens time was supported with funds from Fonds Français pour l'Environnement Mondial through the DynAfFor Project and also with the fund from the World Bank throughout the PreREDD+ Project. We also thank the ngo Nature + for their administrative support.

Data accessibility

The original photogrammetric point clouds and the destructive sampling data are available through ORBI (http://hdl.handle.net/2268/202113) .

References

Alder, D. & Synnott, T.J. (1992) *Permanent Sample Plot Techniques for Mixed Tropical Forest*. Tropical forestry papers, Oxford Forestry Institute, Oxford, UK. No. 25, 124 p.

Antin, C., Pélissier, R., Vincent, G. & Couteron, P. (2013) Crown allometries are less responsive than stem allometry to tree size and habitat variations in an Indian monsoon forest. *Trees*, **27**, 1485–1495.

Banin, L., Feldpausch, T.R., Phillips, O.L. *et al*. (2012) What controls tropical forest architecture? Testing environmental, structural and floristic drivers. *Global Ecology and Biogeography*, **21**, 1179–1190.

Banin, L., Leis, S.L., Lopez-Gonzalez, G. *et al*. (2014) Tropical forest wood production: a cross-continental comparison. *Journal of Ecology*, **102**, 1025–1037.

Barazzetti, L., Scaioni, M. & Remondino, F. (2010) Orientation and 3D modelling from markerless terrestrial images: combining accuracy with automation. *The Photogrammetric Record*, **25**, 356–381.

Baskerville, G.L. (1972) Use of logarithmic regression in the estimation of plant biomass. *Canadian Journal of Forest Research*, **2**, 49–53.

Bastin, J.F., Barbier, N., Réjou-Méchain, M. *et al*. (2015) Seeing Central African forests through their largest trees. *Scientific Reports*, **5**, 13156.

Belyea, H.C. (1931) *Forest Measurement*. Wiley & Sons, New York, NY, USA; Chapman & Hall, London, UK.

Bruce, D. & Schumacher, F.X. (1950) *Forest Mensuration*. McGraw-Hill Book Co., New York, NY, USA.

Cailliez, F. (1980) *Forest Volume Estimation and Yield Prediction – Volume Estimation*. F.A.O, Forestry Paper 22/1, Rome, Italy, 98p.

Chapman, C.A., Kaufman, L. & Chapman, L.J. (1998) Buttress formation and directional stress experienced during critical phases of tree development. *Journal of Tropical Ecology*, **14**, 341–349.

Chave, J., Andalo, C., Brown, S. *et al*. (2005) Tree allometry and improved estimation of carbon stocks and balance in tropical forests. *Oecologia*, **145**, 87–99.

Chave, J., Rejou-Mechain, M., Burquez, A. *et al.* (2014) Improved allometric models to estimate the aboveground biomass of tropical trees. *Global Change Biology*, **20**, 3177–3190.
Clark, D.A. (2002) Are tropical forests an important carbon sink? Reanalysis of the long-term plot data. *Ecological Applications*, **12**, 3–7.
Clark, D.A. & Clark, D.B. (1999) Assessing the growth of tropical rain forest trees: issues for forest modeling and management. *Ecological Applications*, **9**, 981–997.
Condit, R. (1998) *Tropical Forest Census Plots: Methods and Results From Barro Colorado Island, Panama and a Comparison With Other Plots*. Springer-Verlag, Berlin, Germany.
Coomes, D.A., Burslem, D.F. & Simonson, W.D. (2014) *Forests and Global Change*. Cambridge University Press, Cambrige, UK.
Cushman, K.C., Muller-Landau, H.C., Condit, R.S. & Hubbell, S.P. (2014) Improving estimates of biomass change in buttressed trees using tree taper models. *Methods in Ecology and Evolution*, **5**, 573–582.
Dean, C. (2003) Calculation of wood volume and stem taper using terrestrial single image close-range photogrammetry and contemporary software tools. *Silva Fennica*, **37**, 359–380.
Dean, C. & Roxburgh, S. (2006) Improving visualisation of mature, high-carbon sequestering forests. *Forest Biometry, Modelling and Information Sciences*, **1**, 48–69.
Dean, C., Roxburgh, S. & Mackey, B.G. (2003) Growth modelling of *Eucalyptus regnans* for carbon accounting at the landscape scale. *Modelling Forest Systems* (eds A. Amaro, D. Reed & P. Soares), pp. 27–39. CABI, Cambrige, UK.
Fayolle, A., Doucet, J.-L., Gillet, J.-F., Bourland, N. & Lejeune, P. (2013a) Tree allometry in Central Africa: testing the validity of pantropical multi-species allometric equations for estimating biomass and carbon stocks. *Forest Ecology and Management*, **305**, 29–37.
Fayolle, A., Rondeux, J., Doucet, J.-L., Ernst, G., Bouissou, C., Quevauvillers, S., Bourland, N., Feteke, F. & Lejeune, P. (2013b) Réviser les tarifs de cubage pour mieux gérer les forêts du Cameroun. *Bois et Forêts des Tropiques*, **317**, 35–49.
Fayolle, A., Picard, N., Doucet, J.-L., Swaine, M., Bayol, N., Bénédet, F. & Gourlet-Fleury, S. (2014) A new insight in the structure, composition and functioning of central African moist forests. *Forest Ecology and Management*, **329**, 195–205.
Feldpausch, T.R., Banin, L., Phillips. *et al.* (2011) Height-diameter allometry of tropical forest trees. *Biogeosciences*, **8**, 1081–1106.
Forbes, R.D. & Meyer, A.B. (1955) *Forestry Handbook*. Ronald Press Company, New York, NY, USA.
Fraser, C.S. & Al-Ajlouni, S. (2006) Zoom-dependent camera calibration in digital close-range photogrammetry. *Photogrammetric Engineering & Remote Sensing*, **72**, 1017–1026.
Goodman, R.C., Phillips, O.L. & Baker, T.R. (2014) The importance of crown dimensions to improve tropical tree biomass estimates. *Ecological Applications*, **24**, 680–698.
Gourlet-Fleury, S., Mortier, F., Fayolle, A., Baya, F., Ouedraogo, D., Benedet, F. & Picard, N. (2013) Tropical forest recovery from logging: a 24 year silvicultural experiment from Central Africa. *Philosophical Transactions of the Royal Society of London B: Biological Sciences*, **368**, 20120302.
He, Z., Tang, Y., Deng, X. & Cao, M. (2012) Buttress trees in a 20-hectare tropical dipterocarp rainforest in Xishuangbanna, SW China. *Journal of Plant Ecology*, **6**, 187–192.
Henry, M., Besnard, A., Asante, W.A., Eshun, J., Adu-Bredu, S., Valentini, R., Bernoux, M. & Saint-Andre, L. (2010) Wood density, phytomass variations within and among trees, and allometric equations in a tropical rainforest of Africa. *Forest Ecology and Management*, **260**, 1375–1388.
Kearsley, E., de Haulleville, T., Hufkens. *et al.* (2013) Conventional tree height-diameter relationships significantly overestimate aboveground carbon stocks in the Central Congo Basin. *Nature communications*, **4**, 2269.
Läbe, T. & Förstner, W. (2004) Geometric stability of low-cost digital consumer cameras. *Proceedings of the 20th ISPRS Congress*, Istanbul, Turkey, pp. 528–535.
Letouzey, R. (1982) *Manuel de Botanique Tropicale – Afrique Tropicale: Tome 1*. Centre Technique Forestier Tropical, Nogent sur Marne, France.
Liang, X., Jaakkola, A., Wang, Y., Hyyppä, J., Honkavaara, E., Liu, J. & Kaartinen, H. (2014) The use of a hand-held camera for individual tree 3D Mapping in forest sample plots. *Remote Sensing*, **6**, 6587–6603.
Mehedi, M.A.H., Kundu, C. & Chowdhury, M.Q. (2012) Patterns of tree buttressing at Lawachara National Park, Bangladesh. *Journal of Forestry Research*, **23**, 461–466.
Metcalf, C.J.E., Clark, J.S. & Clark, D.A. (2009) Tree growth inference and prediction when the point of measurement changes: modelling around buttresses in tropical forests. *Journal of Tropical Ecology*, **25**, 1–12.
Meunier, Q., Moumbogou, C. & Doucet, J.-L. (2015) *Les Arbres Utiles du Gabon*. Presses Agronomiques de Gembloux, Gembloux, Belgium.
Muller-Landau, H.C., Detto, M., Chisholm, R.A., Hubbell, S.P. & Condit, R. (2014) Detecting and projecting changes in forest biomass from plot data. *Forests and Global Change* (eds D.A. Coomes, D.F.R.P. Burslem & W.D. Simonson), pp. 381–416. Cambridge University Press, Cambridge, UK.
Ngomanda, A., Mavouroulou, Q.M., Obiang, N.L.E., Iponga, D.M., Mavoungou, J.-F., Lepengue, N., Picard, N. & Mbatchi, B. (2012) Derivation of diameter measurements for buttressed trees, an example from Gabon. *Journal of Tropical Ecology*, **28**, 299–302.
Nogueira, E.M., Nelson, B.W. & Fearnside, P.M. (2006) Volume and biomass of trees in central Amazonia: influence of irregularly shaped and hollow trunks. *Forest Ecology and Management*, **227**, 14–21.
Nölke, N., Fehrmann, L., I Nengah, S.J., Tiryana, T., Seidel, D. & Kleinn, C. (2015) On the geometry and allometry of big-buttressed trees – a challenge for forest monitoring: new insights from 3D-modeling with terrestrial laser scanning. *iForest-Biogeosciences and Forestry*, **8**, 574–581.
Pan, Y., Birdsey, R.A., Fang, J. *et al.* (2011) A large and persistent carbon sink in the world's forests. *Science*, **333**, 988–993.
Phillips, O.L., Baker, T.R., Brienen, R. & Feldpausch, T.R. (2015) *Field manual for plot establishment and remeasurement*. http://www.rainfor.org/en/manuals.
Picard, N. & Gourlet-Fleury, S. (2008) *Manuel de Référence Pour L'installation de Dispositifs Permanents en Forêt de Production Dans le Bassin du Congo*. COMIFAC, Yaounde, Cameroon.
Ploton, P., Barbier, N., Takoudjou Momo, S. *et al.* (2016) Closing a gap in tropical forest biomass estimation: taking crown mass variation into account in pantropical allometries. *Biogeosciences*, **13**, 1571–1585.
Plumptre, A.J. (1995) The importance of "seed trees" for the natural regeneration of selectively logged tropical forest. *The Commonwealth Forestry Review*, **25**, 3–258.
Pulkkinen, M. (2012) On non-circularity of tree stem cross-sections: effect of diameter selection on cross-section area estimation, Bitterlich sampling and stem volume estimation in Scots pine. *Silva Fennica*, **46**, 747–986.
Rondeux, J. (1993) *La Mesure des Arbres et des Peuplements Forestiers*. Les presses agronomiques de Gembloux, Gembloux, Belgium.
Shortis, M.R., Bellman, C.J., Robson, S., Johnston, G.J. & Johnson, G.W. (2006) Stability of zoom and fixed lenses used with digital SLR cameras. *Proceedings of the ISPRS Commission V Symposium of Image Engineering and Vision Metrology*, Citeseer, pp. 285–290.
Slik, J.W., Paoli, G., McGuire, K. *et al.* (2013) Large trees drive forest aboveground biomass variation in moist lowland forests across the tropics. *Global Ecology and Biogeography*, **22**, 1261–1271.
Sprugel, D.G. (1983) Correcting for bias in log-transformed allometric equations. *Ecology*, **64**, 209–210.
Swaine, M.D., Lieberman, D. & Putz, F.E. (1987) The dynamics of tree populations in tropical forest: a review. *Journal of Tropical Ecology*, **3**, 359–366.
Szeliski, R. (2010) *Computer Vision: Algorithms and Applications*. Springer-Verlag, London Limited, London, UK.
Thompson, J., Proctor, J., Viana, V., Milliken, W., Ratter, J.A. & Scott, D.A. (1992) Ecological studies on a lowland evergreen rain forest on Maraca Island, Roraima, Brazil. I. Physical environment, forest structure and leaf chemistry. *Journal of Ecology*, **80**, 689–703.
Wenzel, K., Rothermel, M., Fritsch, D. & Haala, N. (2013) Image acquisition and model selection for multi-view stereo. *ISPRS-International Archives of the Photogrammetry, Remote Sensing and Spatial Information Sciences*, **1**, 251–258.

Received 31 May 2016; accepted 12 September 2016
Handling Editor: Sean McMahon

Supporting Information

Additional Supporting Information may be found online in the supporting information tab for this article:

Appendix S1. Description of the Loundoungou site (Republic of Congo).

Appendix S2. Methodology and validation of the photogrammetric process.

Appendix S3. POM definition, formatting biomass data and $D_{area130}$-field variable relationships.